

## Supporting Information

### Pyramidal Nd<sub>2</sub>ScN Inside the Icosahedral C<sub>80</sub> Cage

Wei Yang,<sup>b</sup> Yaofeng Wang,<sup>b</sup> Alexey A. Popov,<sup>b\*</sup> Fupin Liu<sup>a\*</sup>

a. Jiangsu Key Laboratory of New Power Batteries, Jiangsu Collaborative Innovation Center of Biomedical Functional Materials, School of Chemistry and Materials Science, Nanjing Normal University, Nanjing 210023, China

b. Leibniz Institute for Solid State and Materials Research (IFW Dresden), Helmholtzstr. 20, 01069, Dresden, Germany

E-mail: a.popov@ifw-dresden.de; liu\_fupin@nnu.edu.cn

### Contents

|  |           |
|--|-----------|
| <b>1. Experimental details .....</b>   | <b>2</b>  |
| <b>2. Separation procedure and mass spectrum of Nd<sub>2</sub>ScN@C<sub>80</sub>.....</b>                                      | <b>3</b>  |
| <b>3. UV-vis-NIR absorption spectrum of Nd<sub>2</sub>ScN@C<sub>80</sub>.....</b>  | <b>4</b>  |
| <b>4. Crystal data.....</b>  | <b>5</b>  |
| <b>5. The fullerene in the crystal lattice. ....</b>   | <b>6</b>  |
| <b>6. The fullerene fragments coordinate with metal ions. ....</b>   | <b>7</b>  |
| <b>7. Nd<sub>2</sub>ScN cluster position relative to the NiOEP .....</b>   | <b>7</b>  |
| <b>8. Distance between N and C<sub>80</sub> centroid and other structural parameters of M<sub>3</sub>N@C<sub>80</sub>.....</b> | <b>8</b>  |
| <b>9. N out of C<sub>80</sub> centroid.....</b>  | <b>9</b>  |
| <b>10. The ordered nitrogen model and the structural parameters.....</b>   | <b>9</b>  |
| <b>11. References .....</b>  | <b>10</b> |

## 1. Experimental details

**Synthesis:** Nd<sub>2</sub>ScN@C<sub>80</sub> was successfully synthesized by direct current arc discharge method with guanidinium thiocyanate as a selective nitrogen source.<sup>1, 2</sup> Specifically, a mixture of Nd<sub>2</sub>O<sub>3</sub>, Sc<sub>2</sub>O<sub>3</sub>, guanidine thiocyanate (GT, C<sub>2</sub>H<sub>6</sub>N<sub>4</sub>S), and graphite powder (C) with the molar ratio of Nd:Sc:GT:C = 1:0.5:2.5:7.5 was filled into the core-drilled graphite rods, which were then evaporated in 180 mbar He atmosphere with a direct current of 100 A. Endohedral metallofullerenes were Soxhlet-extracted from the synthesized soot by CS<sub>2</sub> and separated by high-performance liquid chromatography (HPLC) using toluene as mobile phase. The absolute yield of metallofullerene synthesis is extremely low. Overall, with input of ca. 50 g of graphite, 45 g of GT, 5 g of Sc<sub>2</sub>O<sub>3</sub> and 26 g of Nd<sub>2</sub>O<sub>3</sub>, roughly 0.3 mg of Nd<sub>2</sub>ScN@C<sub>80</sub> and 1.5 mg of NdSc<sub>2</sub>N@C<sub>80</sub> were obtained.

**HPLC:** HPLC separation was performed for toluene solutions of fullerene and with toluene as an eluent, employing semipreparative COSMOSIL Buckyprep chromatographic column (Nacalai Tesque) and Agilent 1260 Infinity II LC System. Recycling HPLC separation was performed using Sunflow 100 system (SunChrome).

**MS:** Laser desorption/ionization time-of-flight (LDI-TOF) mass spectra were measured with a Bruker autoflex mass spectrometer.

**UV-Vis-NIR:** UV-vis-NIR absorption spectra were measured in carbon disulfide solution at room temperature with Shimadzu 3100 spectrophotometer.

**X-ray diffraction:** single crystal X-ray diffraction data collection was carried out at the BESSY storage ring (BL14.2, Berlin-Adlershof, Germany).<sup>3</sup> XDSAPP2.0 suite was employed for data processing.<sup>4, 5</sup> The structure was solved by direct methods and refined by SHELXL-2018.<sup>6</sup> Hydrogen atoms were added geometrically and refined with a riding model. The crystal data are presented in Table S1 in the supporting information. For the disorder model of metal atoms, we first refined all 9 possible positions of metal atoms by applying the heavy Nd with free site occupancy developed by us previously.<sup>7</sup> The site occupancies shows a pattern of three rigid Nd<sub>2</sub>Sc sites, with two Nd positions show similar occupancy and the other one significantly lower occupancy. So, we finally refine the structure with three sites with the low occupancy Nd site replaced with Sc. Because the resulted site occupancies in the main site (Nd1, Nd2, and Sc1) are very similar, so we set the site occupancy for Nd1, Nd2, and Sc1 as equal. Similarly, we refined the remaining two sites Nd3, Nd4, and Sc2 as well as Nd5, Nd6, and Sc3.

## 2. Separation procedure and mass spectrum of $\text{Nd}_2\text{ScN}@\text{C}_{80}$

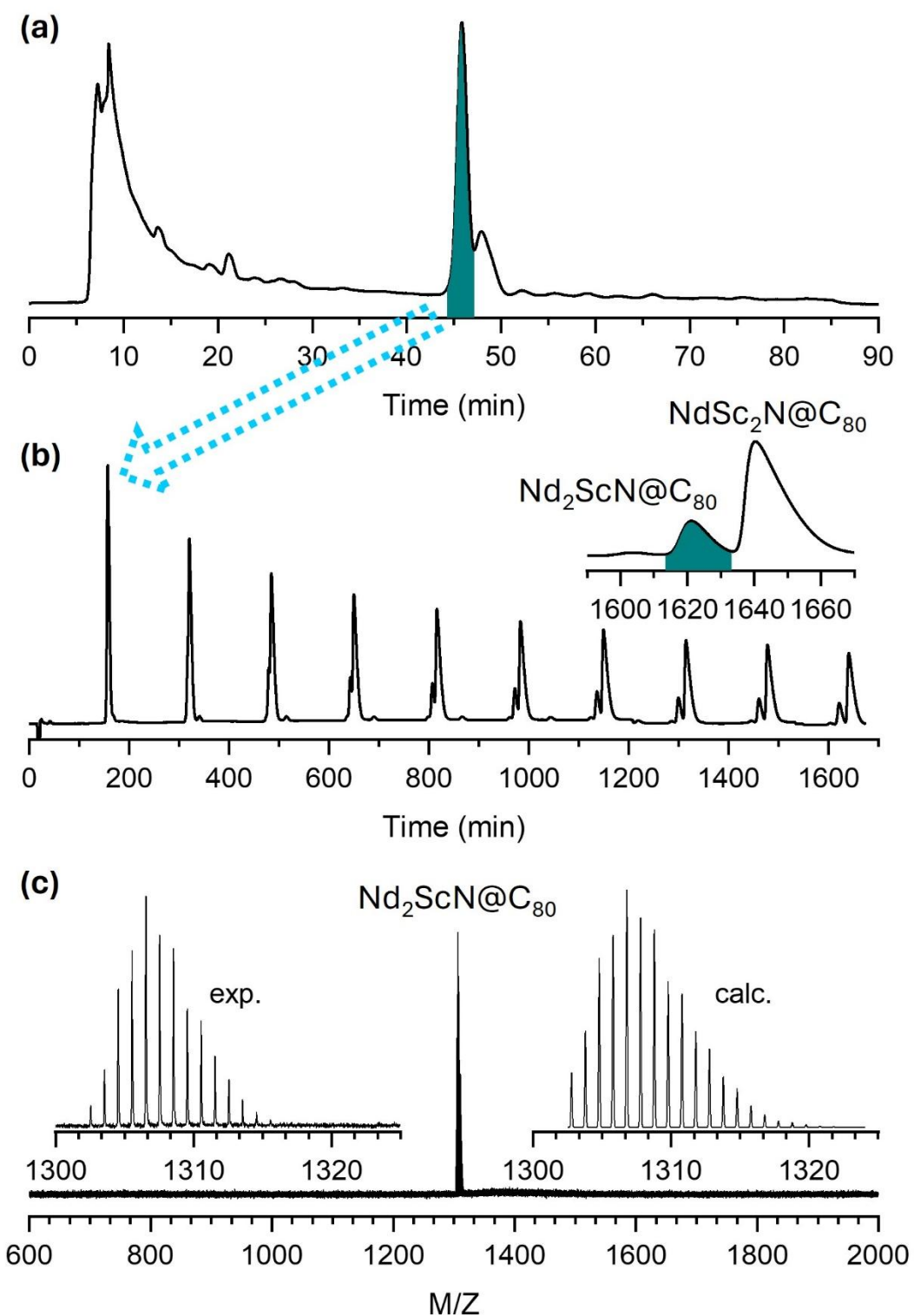


**Figure S1.** Separation of  $\text{Nd}_2\text{ScN}@C_{80}$ . (a) HPLC profile of first step separation applying two linearly connected Buckyprep columns with toluene as mobile phase at a flow rate of 5mL/min.

The highlighted fraction was collected for the second step separation (b) by applying one Buckyprep column at a flow rate of 1mL/min with recycling mode. The highlighted fraction was collected and identified with laser desorption ionization mass spectrometry as  $\text{Nd}_2\text{ScN}@C_{80}$  (c).

### 3. UV-vis-NIR absorption spectrum of $\text{Nd}_2\text{ScN}@\text{C}_{80}$

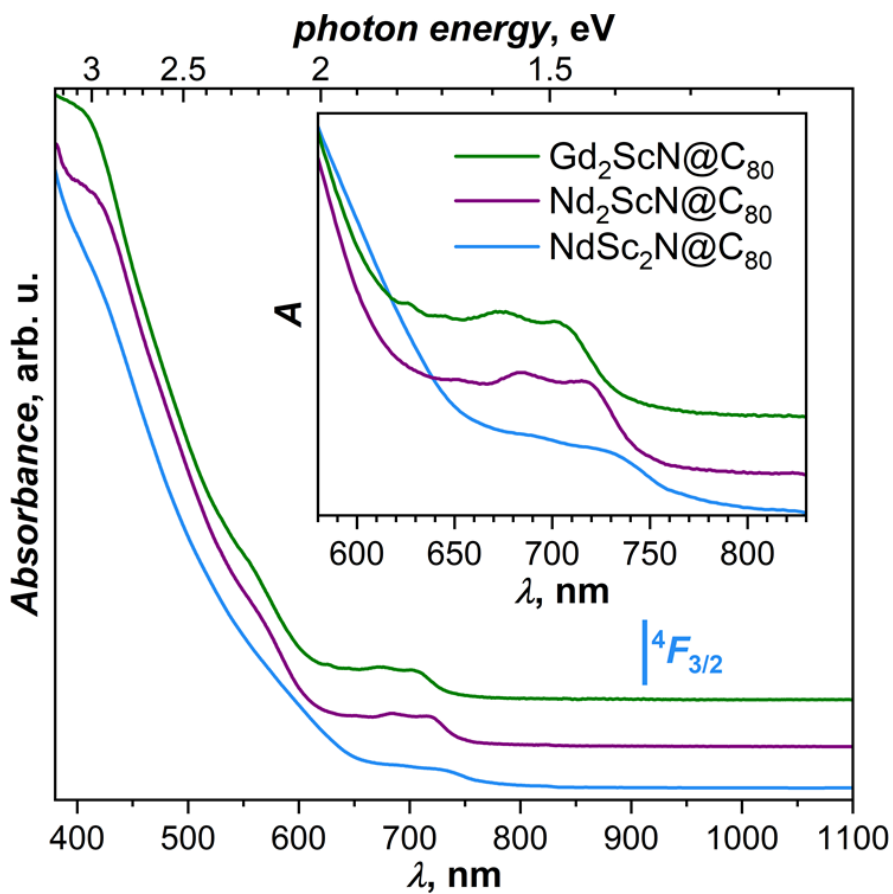


**Figure S2.** UV-vis-NIR absorption spectrum of  $\text{Nd}_2\text{ScN}@\text{C}_{80}$  measured in  $\text{CS}_2$  solution compared to the spectra of  $\text{NdSc}_2\text{N}@\text{C}_{80}$  and  $\text{Gd}_2\text{ScN}@\text{C}_{80}$ ; inset shows enhancement of the low-energy range. The vertical bar marks the energy of the  $\text{Nd}^{3+}$ -emitting state  $^4F_{3/2}$  in  $\text{NdSc}_2\text{N}@\text{C}_{80}$ . Note that low-energy absorptions of  $\text{Nd}_2\text{ScN}@\text{C}_{80}$  are blue-shifted from  $\text{NdSc}_2\text{N}@\text{C}_{80}$  and better resolved than in the latter. The spectrum of  $\text{Nd}_2\text{ScN}@\text{C}_{80}$  is similar to the spectra of other  $\text{M}_2\text{ScN}@c_{80}$ , exemplified here with  $\text{Gd}_2\text{ScN}@\text{C}_{80}$ .

#### 4. Crystal data

**Table S1. Crystal data\_Nd<sub>2</sub>ScN@C<sub>80</sub>.**

|  |   |
|--|---|
| <b>Crystal</b>                                   | Nd <sub>2</sub> ScN@C <sub>80</sub> ·NiOEP·2C <sub>6</sub> H <sub>6</sub> |
| <b>Formula</b>                                   | C <sub>128</sub> H <sub>56</sub> N <sub>5</sub> Nd <sub>2</sub> NiSc      |
| <b>Formula weight</b>                            | 2055.74   |
| <b>Color, habit</b>                              | Black, block  |
| <b>Crystal system</b>                            | monoclinic  |
| <b>Space group</b>                               | C2/c  |
| <b>a, Å</b>                                      | 25.270(5)   |
| <b>b, Å</b>                                      | 15.030(3)   |
| <b>c, Å</b>                                      | 39.450(8)   |
| <b>α, deg</b>                                    | 90  |
| <b>β, deg</b>                                    | 95.41(3)  |
| <b>γ, deg</b>                                    | 90  |
| <b>Volume, Å<sup>3</sup></b>                     | 14917(5)  |
| <b>Z</b>   | 8   |
| <b>T, K</b>                                      | 100   |
| <b>Radiation (λ, Å)</b>                          | Synchrotron Radiation (0.77977)   |
| <b>Unique data (R<sub>int</sub>)</b>             | 24019 (0.0581)  |
| <b>Parameters</b>                                | 1330  |
| <b>Restraints</b>                                | 104   |
| <b>Observed data (I &gt; 2σ(I))</b>              | 23181   |
| <b>R<sub>1</sub><sup>a</sup> (observed data)</b> | 0.0435  |
| <b>wR<sub>2</sub><sup>b</sup> (all data)</b>     | 0.1243  |
| <b>CCDC NO.</b>                                  | 2351764   |

<sup>a</sup>For data with  $I > 2\sigma(I)$ ,  $R_1 = \frac{\sum|F_o - |F_c||}{\sum|F_o|}$ . <sup>b</sup>For all data,  $wR_2 = \sqrt{\frac{\sum[w(F_o^2 - F_c^2)^2]}{\sum[w(F_o^2)^2]}}$ .

## 5. The fullerene in the crystal lattice.

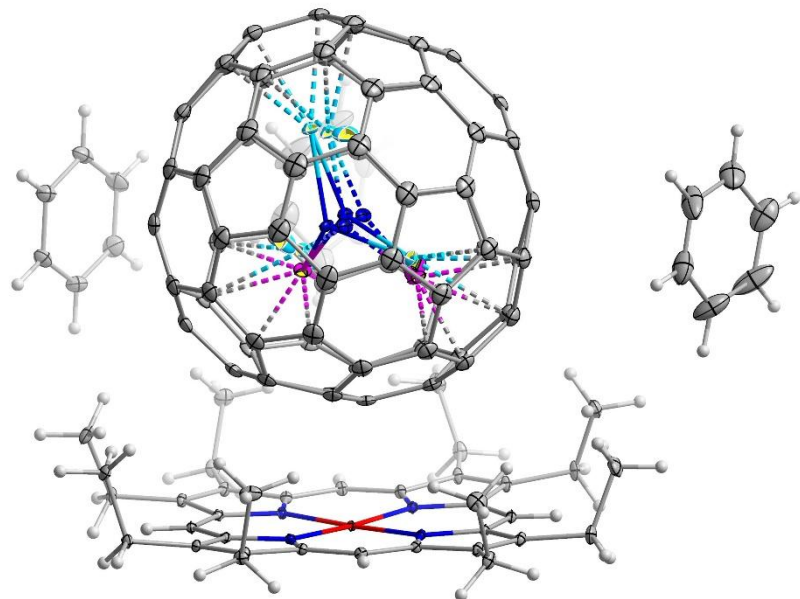


**Figure S3.** The structure of  $\text{Nd}_2\text{ScN}@C_{80} \cdot \text{NiOEP} \cdot 2\text{C}_6\text{H}_6$  with all molecules in the asymmetric unit. Color code: gray for C, white for H, blue for N, red for Ni, pink for Sc, and cyan for Nd. The thermal ellipsoids are set at 30% probability.

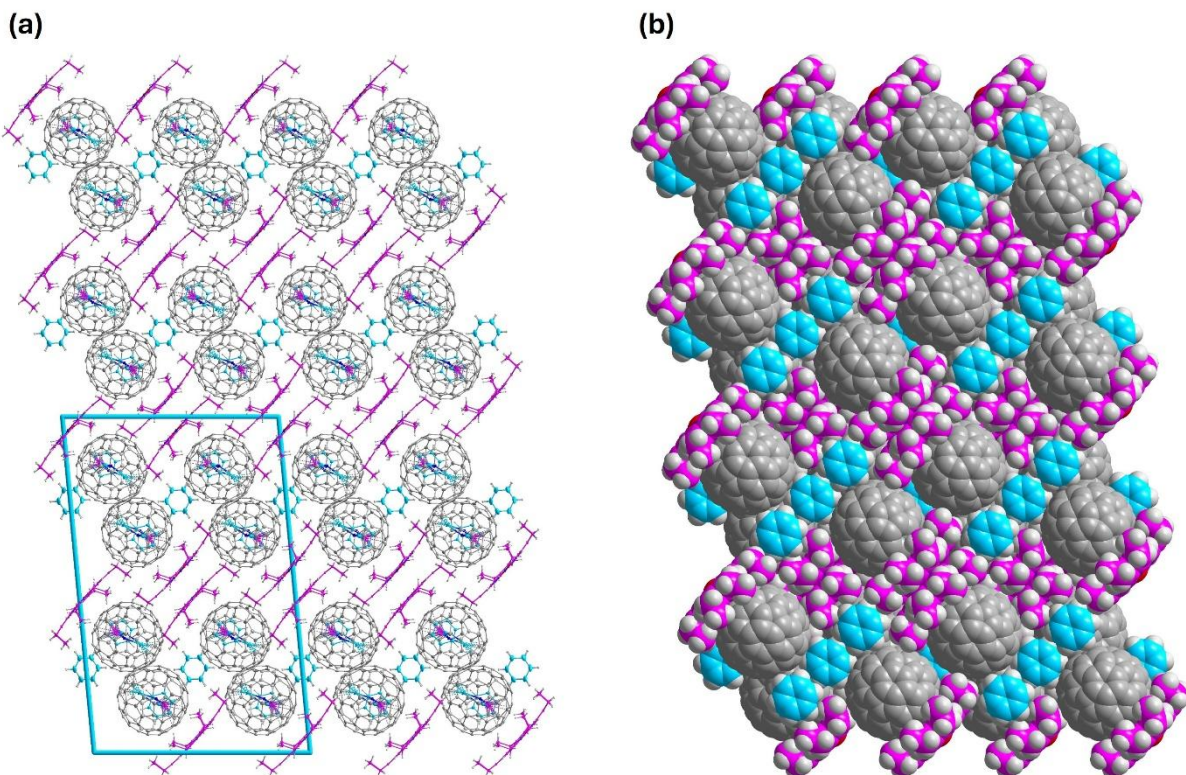


**Figure S4.** The structure of  $\text{Nd}_2\text{ScN}@C_{80} \cdot \text{NiOEP} \cdot 2\text{C}_6\text{H}_6$  with the packing of molecules in the crystal lattice with the ball-stick model in (a) and the space-filling model in (b). Color code: gray for the C of the fullerene cages, sky blue for the C of the benzene molecules, pink for the C of the NiOEP, white for H, blue for N, red for Ni, pink for Sc, and cyan for Nd.

## 6. The fullerene fragments coordinate with metal ions.

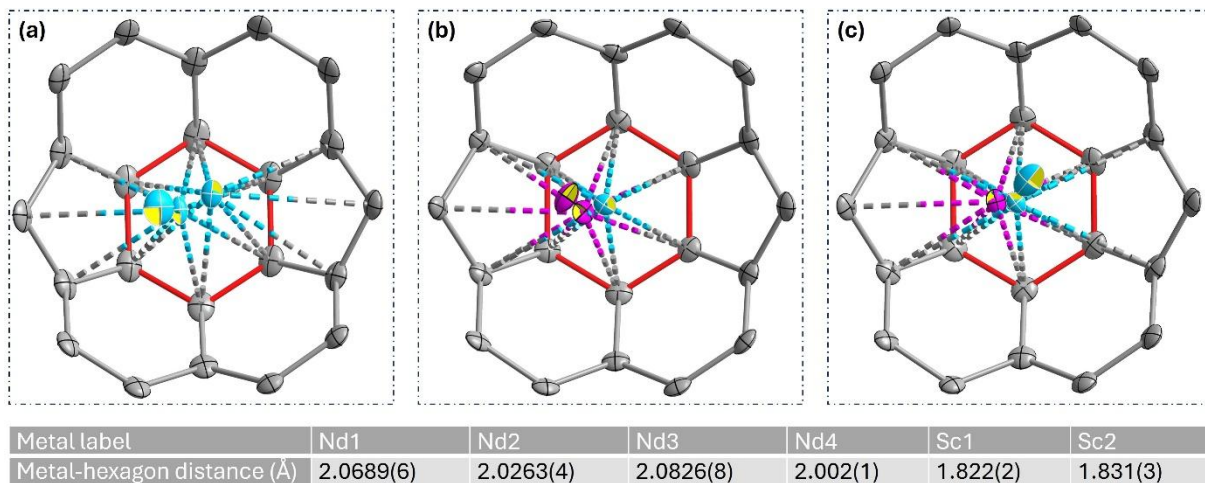


**Figure S5.** The fullerene fragments coordinate with metal ions, (a) Nd1, Nd3, and Nd6, (b) Nd2, Sc2, and Sc3, (c) Sc1, Nd4, and Nd5. Color code: gray for C, pink for Sc, and cyan for Nd. The thermal ellipsoids are set at 30% probability. The coordinating hexagon was highlighted with red bonds. The metal-to-hexagonal plane distances were compiled in the figure.

## 7. Nd<sub>2</sub>ScN cluster position relative to the NiOEP

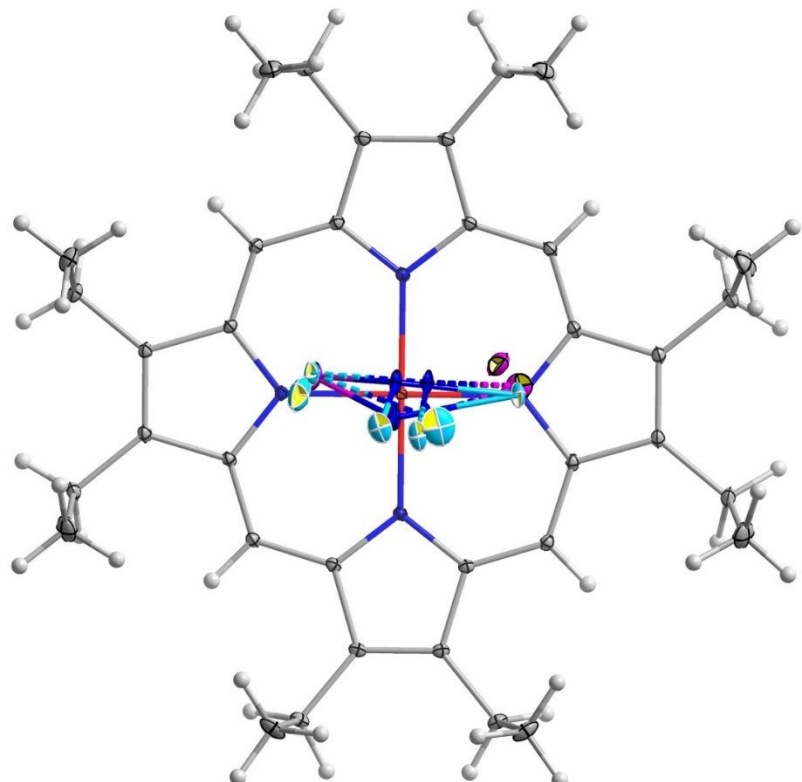


**Figure S6.** The structure of Nd<sub>2</sub>ScN@C<sub>80</sub>·NiOEP·2C<sub>6</sub>H<sub>6</sub> viewed perpendicular to the NiOEP plane. The structures are shown without C<sub>80</sub> and solvents for clarity to present the metal positions.

## 8. Distance between N and C<sub>80</sub> centroid and other structural parameters of M<sub>3</sub>N@C<sub>80</sub>.

**Table S2. The reported distance between N and C<sub>80</sub> centroid of M<sub>3</sub>N@C<sub>80</sub> determined by single crystal X-ray diffraction with the co-crystal of fullerene-NiOEP**

| M <sub>3</sub> N@C <sub>80</sub>        | M-N bond lengths (Å)           | N-C <sub>80</sub> centroid distance (Å) | N-M <sub>3</sub> plane distance (Å)    | Ref.         |
|---|--------------------------------|---|--|--------------|
| <b>ScV<sub>2</sub>N@C<sub>80</sub></b>  | 2.003(6)/ 1.995(5)/ 2.027(3)   | 0.044(6)                                | 0.008(8)                               | 8            |
| <b>Sc<sub>2</sub>VN@C<sub>80</sub></b>  | 2.036(4)/ 2.036(4)/ 1.858(7)   | 0.133(8)                                | 0.119(8)                               | 8            |
| <b>Sc<sub>3</sub>N@C<sub>80</sub></b>   | 2.022(3)/ 2.010(3)/ 2.034(4)   | 0.022(2)                                | 0.103(3)                               | 9            |
| <b>ErSc<sub>2</sub>N@C<sub>80</sub></b> | 2.089(9)/ 1.968(6)/ 1.968(6)   | 0.162                                   | 0.08(1)                                | 10           |
| <b>DySc<sub>2</sub>N@C<sub>80</sub></b> | 2.096(6) / 1.965(6) / 1.978(6) | 0.201(6)                                | 0.040(6)                               | 11           |
| <b>Dy<sub>2</sub>ScN@C<sub>80</sub></b> | 1.95(2)/ 2.07(2)/ 2.079(5)     | 0.19(1)/ 0.30(6)                        | 0.012(5)                               | 12           |
| <b>TbSc<sub>2</sub>N@C<sub>80</sub></b> | 2.13(2)/ 1.949(8)/ 1.949(8)    | 0.22(2)                                 | 0.02(2)                                | 13           |
| <b>GdSc<sub>2</sub>N@C<sub>80</sub></b> | 2.15(1)/ 1.916(9)/ 1.919(8)    | 0.2614(1)                               | 0.0092(2)                              | 13           |
| <b>Gd<sub>2</sub>ScN@C<sub>80</sub></b> | 2.072(3)/ 2.100(3)/ 1.900(4)   | 0.229(3)                                | 0.023(3)                               | 13           |
| <b>NdSc<sub>2</sub>N@C<sub>80</sub></b> | 2.170(2)/ 1.951(2)/ 1.944(2)   | 0.320(2)                                | 0.031(2)                               | 14           |
| <b>Nd<sub>2</sub>ScN@C<sub>80</sub></b> | 2.108(4)/ 2.132(5)/ 1.907(5)   | 0.41(2)/ 0.448(6)/<br>0.41(2)/ 0.44(1)  | 0.29(2)/ 0.322(6)/<br>0.28(2)/ 0.28(2) | this<br>work |
| <b>CeSc<sub>2</sub>N@C<sub>80</sub></b> | 2.184(2)/ 1.942(2)/ 1.933(2)   | 0.360(3)                                | 0.010(3)                               | 15           |
| <b>LaSc<sub>2</sub>N@C<sub>80</sub></b> | 2.196(4)/ 1.943(6) / 1.921(7)  | 0.389(4)                                | 0.007(4)                               | 16           |
| <b>Lu<sub>3</sub>N@C<sub>80</sub></b>   | 2.022(8)/ 2.072(8)/ 2.048(8)   | 0.035(8)                                | 0.011(8)                               | 17           |
| <b>Lu<sub>3</sub>N@C<sub>80</sub></b>   | 2.021(5)/ 2.053(2)/ 2.048(6)   | 0.041(7)                                | 0.002(8)                               | 18           |
| <b>Tm<sub>3</sub>N@C<sub>80</sub></b>   | 2.032(6)/ 2.020(6)/ 2.058(6)   | 0.023(6)                                | 0.012(8)                               | 19           |
| <b>Dy<sub>2</sub>VN@C<sub>80</sub></b>  | 2.088(6)/ 2.088(6)/ 1.84(2)    | 0.34(2)                                 | 0.05(2)                                | 20           |
| <b>Ho<sub>2</sub>LuN@C<sub>80</sub></b> | 2.050(4)/ 2.043(4)/ 2.042(4)   | 0.019(5)                                | 0.006(5)                               | 17           |
| <b>Er<sub>3</sub>N@C<sub>80</sub></b>   | 2.046(3)/ 2.059(3)/ 2.028(3)   | 0.007(3)                                | 0.025(3)                               | 21           |
| <b>Ho<sub>3</sub>N@C<sub>80</sub></b>   | 2.015(8)/ 2.057(8)/ 2.051(8)   | 0.034(8)                                | 0.058(9)                               | 21           |
| <b>DyErScN@C<sub>80</sub></b>           | 1.965(4)/ 2.019(5)/ 1.959(3)   | 0.072(3)                                | 0.205(3)                               | 22           |
| <b>DyEr<sub>2</sub>N@C<sub>80</sub></b> | 2.01(1)/ 2.05(1)/ 2.05(1)      | 0.05(2)                                 | 0.05(2)                                | 23           |
| <b>Y<sub>3</sub>N@C<sub>80</sub></b>    | 2.028(3)/ 2.042(3)/ 2.057(3)   | 0.017(3)                                | 0.011(4)                               | 7            |
| <b>Y<sub>2</sub>DyN@C<sub>80</sub></b>  | 2.046(2)/ 2.028(2)/ 2.043(2)   | 0.009(3)                                | 0.013(3)                               | 7            |
| <b>YDy<sub>2</sub>N@C<sub>80</sub></b>  | 2.004(4)/ 2.021(4)/ 2.078(4)   | 0.029(5)                                | 0.038(5)                               | 7            |
| <b>Dy<sub>3</sub>N@C<sub>80</sub></b>   | 2.049(3)/ 2.019(3)/ 2.041(3)   | 0.019(5)                                | 0.018(6)                               | 7            |
| <b>Dy<sub>3</sub>N@C<sub>80</sub></b>   | 2.004(8)/ 2.068(6)/ 2.055(7)   | 0.064(9)                                | 0.07(2)                                | 24           |
| <b>CeLu<sub>2</sub>N@C<sub>80</sub></b> | 2.080(7)/ 2.016(7)/ 2.061(8)   | 0.37(1)/ 0.356(9)                       | 0.349(8)/ 0.325(8)                     | 25           |
| <b>Tb<sub>3</sub>N@C<sub>80</sub></b>   | 2.056(4)/ 2.089(4)/ 2.077(4)   | 0.440(5)/ 0.418(7)                      | 0.453(4)/ 0.405(7)                     | 26           |
| <b>DyGd<sub>2</sub>N@C<sub>80</sub></b> | 2.03(1)/ 2.08(1)/ 2.10(2)      | 0.45(2)/ 0.46(2)                        | 0.46(2)/ 0.45(2)                       | 23           |
| <b>Gd<sub>3</sub>N@C<sub>80</sub></b>   | 2.038(8)/ 2.085(4)/ 2.117(5)   | 0.5112/ 0.4842                          | 0.522(8)/ 0.46(2)                      | 27           |
| <b>Dy<sub>2</sub>LaN@C<sub>80</sub></b> | 2.095(4)/ 2.082(3)/ 2.118(5)   | 0.597(3)/ 0.570(9)                      | 0.619(4)/ 0.530(9)                     | 7            |

## 9. N out of C<sub>80</sub> centroid

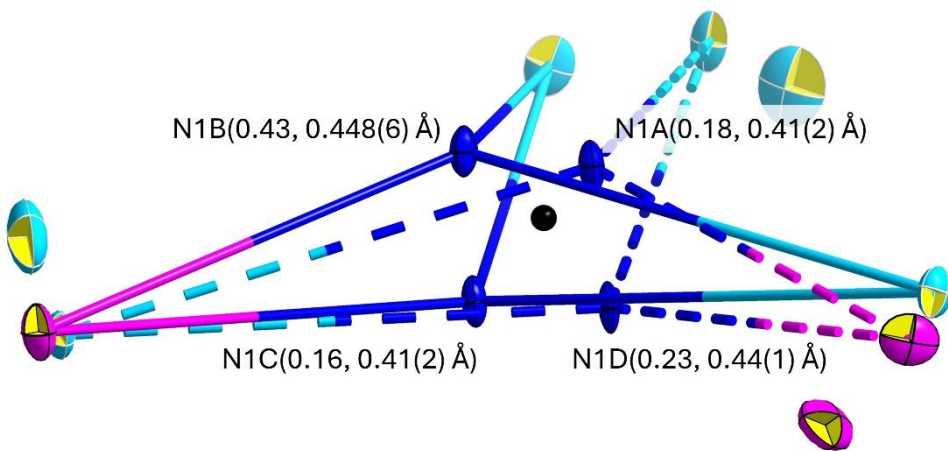


**Figure S7.** Structure of Nd<sub>2</sub>ScN with all positions, the black dot marks the centroid of C<sub>80</sub>. The four N sites were noted with their site occupancies and distances from the C<sub>80</sub> centroid in parentheses. Color code: blue for N, pink for Sc, and cyan for Nd. The thermal ellipsoids are set at 5% probability.

## 10. The ordered nitrogen model and the structural parameters

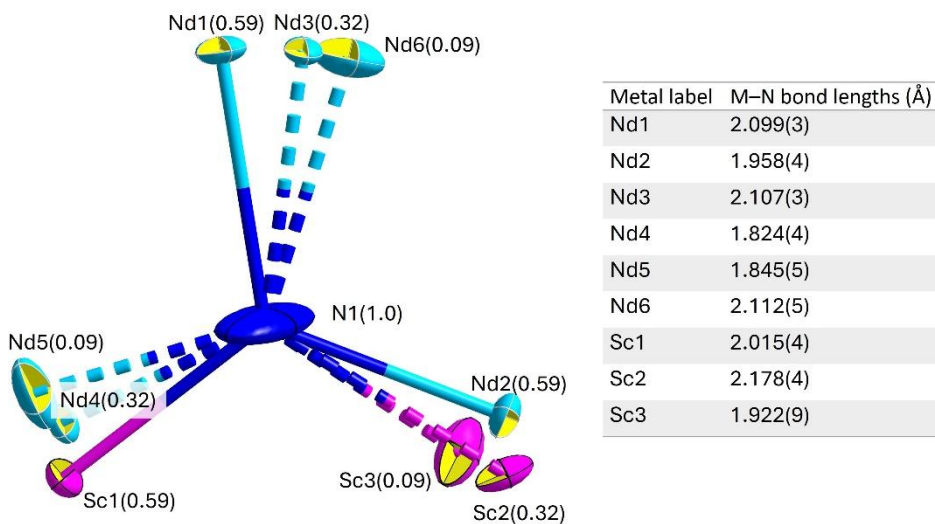


**Figure S8.** Structure of Nd<sub>2</sub>ScN with all positions, one nitrogen position with 1.0 site occupancy was refined. The atoms were noted with the site occupancy in parentheses. Color code: blue for N, pink for Sc, and cyan for Nd. The thermal ellipsoids are set at 30% probability. The M–N bond lengths were compiled in the figure.

## 11. References

1. S. Yang, L. Zhang, W. Zhang and L. Dunsch, A Facile Route to Metal Nitride Clusterfullerenes by Using Guanidinium Salts: A Selective Organic Solid as the Nitrogen Source, *Chem. Eur. J.*, 2010, **16**, 12398-12405.
2. D. S. Krylov, F. Liu, S. M. Avdoshenko, L. Spree, B. Weise, A. Waske, A. U. B. Wolter, B. Büchner and A. A. Popov, Record-high thermal barrier of the relaxation of magnetization in the nitride clusterfullerene  $\text{Dy}_2\text{ScN}@C_{80}-I_h$ , *Chem. Commun.*, 2017, **53**, 7901-7904.
3. U. Mueller, R. Förster, M. Hellmig, F. U. Huschmann, A. Kastner, P. Malecki, S. Pühringer, M. Röwer, K. Sparta, M. Steffien, M. Uhlein, P. Wilk and M. S. Weiss, The macromolecular crystallography beamlines at BESSY II of the Helmholtz-Zentrum Berlin: Current status and perspectives, *Eur. Phys. J. Plus*, 2015, **130**, 141.
4. W. Kabsch, XDS, *Acta Cryst. D*, 2010, **66**, 125-132.
5. K. M. Sparta, M. Krug, U. Heinemann, U. Mueller and M. S. Weiss, XDSAPP2.0, *J. Appl. Cryst.*, 2016, **49**, 1085-1092.
6. G. Sheldrick, Crystal structure refinement with SHELXL, *Acta Cryst. C*, 2015, **71**, 3-8.
7. Y. Hao, G. Velkos, S. Schiemenz, M. Rosenkranz, Y. Wang, B. Büchner, S. Avdoshenko, A. A. Popov and F. Liu, Using internal strain and mass to modulate Dy...Dy coupling and relaxation of magnetization in heterobimetallic metallofullerenes  $\text{DyM}_2\text{N}@C_{80}$  and  $\text{Dy}_2\text{MN}@C_{80}$  ( $\text{M} = \text{Sc}$ ,  $\text{Y}$ ,  $\text{La}$ ,  $\text{Lu}$ ), *Inorg. Chem. Front.*, 2023, **10**, 468-484.
8. T. Wei, S. Wang, X. Lu, Y.-Z. Tan, J. Huang, F. Liu, Q. Li, S. Xie and S. Yang, Entrapping a Group-VB Transition Metal, Vanadium, within an Endohedral Metallofullerene:  $\text{V}_x\text{Sc}_{3-x}\text{N}@I_h-C_{80}$  ( $x=1, 2$ ), *J. Am. Chem. Soc.*, 2016, **138**, 207-214.
9. Y. Hao, Y. Wang, L. Spree and F. Liu, Rotation of fullerene molecules in the crystal lattice of fullerene/porphyrin:  $\text{C}_{60}$  and  $\text{Sc}_3\text{N}@C_{80}$ , *Inorg. Chem. Front.*, 2021, **8**, 122-126.
10. M. M. Olmstead, A. de Bettencourt-Dias, J. C. Duchamp, S. Stevenson, H. C. Dorn and A. L. Balch, Isolation and crystallographic characterization of  $\text{ErSc}_2\text{N}@C_{80}$ : an endohedral fullerene which crystallizes with remarkable internal order, *J. Am. Chem. Soc.*, 2000, **122**, 12220-12226.
11. D. S. Krylov, F. Liu, A. Brandenburg, L. Spree, V. Bon, S. Kaskel, A. U. B. Wolter, B. Büchner, S. M. Avdoshenko and A. A. Popov, Magnetization relaxation in the single-ion magnet  $\text{DySc}_2\text{N}@C_{80}$ : quantum tunneling, magnetic dilution, and unconventional temperature dependence, *Phys. Chem. Chem. Phys.*, 2018, **20**, 11656-11672.
12. Y. Wang and F. Liu, Fullerene rotation dictated by benzene–fullerene interactions, *Inorg. Chem. Front.*, 2024, **11**, 3458-3464.
13. S. Stevenson, C. J. Chancellor, H. M. Lee, M. M. Olmstead and A. L. Balch, Internal and external factors in the structural organization in cocrystals of the mixed-metal endohedrals ( $\text{GdSc}_2\text{N}@I_h-C_{80}$ ,  $\text{Gd}_2\text{ScN}@I_h-C_{80}$ , and  $\text{TbSc}_2\text{N}@I_h-C_{80}$ ) and nickel(II) octaethylporphyrin, *Inorg. Chem.*, 2008, **47**, 1420-1427.
14. W. Yang, M. Rosenkranz, G. Velkos, F. Ziegs, V. Dubrovin, S. Schiemenz, L. Spree, M. F. de Souza Barbosa, C. Guillemand, S. M. Valvidares, B. Büchner, F. Liu, S. Avdoshenko and A. A. Popov, Covalency versus magnetic axiality in Nd molecular magnets: Nd photoluminescence, strong ligand-field, and unprecedented nephelauxetic effect in fullerenes  $\text{NdM}_2\text{N}@C_{80}$  ( $\text{M} = \text{Sc}, \text{Lu}, \text{Y}$ ), *Chem. Sci.*, 2024, **15**, 2141-2157.
15. X. L. Wang, T. M. Zuo, M. M. Olmstead, J. C. Duchamp, T. E. Glass, F. Cromer, A. L. Balch and H. C. Dorn, Preparation and structure of  $\text{CeSc}_2\text{N}@C_{80}$ : An icosahedral carbon cage enclosing an acentric  $\text{CeSc}_2\text{N}$  unit with buried f electron spin, *J. Am. Chem. Soc.*, 2006, **128**, 8884-8889.
16. S. Stevenson, C. B. Rose, J. S. Maslenikova, J. R. Villarreal, M. A. Mackey, B. Q. Mercado, K. Chen, M. M. Olmstead and A. L. Balch, Selective Synthesis, Isolation, and Crystallographic Characterization of  $\text{LaSc}_2\text{N}@I_h-C_{80}$ , *Inorg. Chem.*, 2012, **51**, 13096-13102.

17. F. Liu and L. Spree, Molecular spinning top: visualizing the dynamics of  $M_3N@C_{80}$  with variable temperature single crystal X-ray diffraction, *Chem. Commun.*, 2019, **55**, 13000-13003.
18. W. Shen, L. Bao, S. Hu, X. Gao, Y. Xie, X. Gao, W. Huang and X. Lu, Isolation and Crystallographic Characterization of  $Lu_3N@C_{2n}$  ( $2n = 80-88$ ): Cage Selection by Cluster Size, *Chem. Eur. J.*, 2018, **24**, 16692-16698.
19. T. Zuo, M. M. Olmstead, C. M. Beavers, A. L. Balch, G. Wang, G. T. Yee, C. Shu, L. Xu, B. Elliott, L. Echegoyen, J. C. Duchamp and H. C. Dorn, Preparation and structural characterization of the  $I_h$  and the  $D_{5h}$  isomers of the endohedral fullerenes  $Tm_3N@C_{80}$ : icosahedral  $C_{80}$  cage encapsulation of a trimetallic nitride magnetic cluster with three uncoupled  $Tm^{3+}$  ions, *Inorg. Chem.*, 2008, **47**, 5234-5244.
20. C. Huang, R. Sun, L. Bao, X. Tian, C. Pan, M. Li, W. Shen, K. Guo, B. Wang, X. Lu and S. Gao, A hard molecular nanomagnet from confined paramagnetic 3d-4f spins inside a fullerene cage, *Nat. Commun.*, 2023, **14**, 8443.
21. M. M. Olmstead, T. Zuo, H. C. Dorn, T. Li and A. L. Balch, Metal Ion Size and the Pyramidalization of Trimetallic Nitride Units Inside a Fullerene Cage: Comparisons of the Crystal Structures of  $M_3N@I_h-C_{80}$  ( $M = Gd, Tb, Dy, Ho, Er, Tm, Lu, and Sc$ ) and Some Mixed Metal Counterparts, *Inorg. Chim. Acta* 2017, **468**, 321-326.
22. M. Nie, J. Xiong, C. Zhao, H. Meng, K. Zhang, Y. Han, J. Li, B. Wang, L. Feng, C. Wang and T. Wang, Luminescent single-molecule magnet of metallofullerene  $DyErScN@I_h-C_{80}$ , *Nano Res.*, 2019, **12**, 1727-1731.
23. C. Schlesier, F. Liu, V. Dubrovin, L. Spree, B. Büchner, S. M. Avdoshenko and A. A. Popov, Mixed dysprosium-lanthanide nitride clusterfullerenes  $DyM_2N@C_{80-I_h}$  and  $Dy_2MN@C_{80-I_h}$  ( $M = Gd, Er, Tm, and Lu$ ): synthesis, molecular structure, and quantum motion of the endohedral nitrogen atom, *Nanoscale*, 2019, **11**, 13139-13153.
24. S. Yang, S. I. Troyanov, A. A. Popov, M. Krause and L. Dunsch, Deviation from the planarity - a large  $Dy_3N$  cluster encapsulated in an  $I_h$ - $C_{80}$  cage: An X-ray crystallographic and vibrational spectroscopic study, *J. Am. Chem. Soc.*, 2006, **128**, 16733-16739.
25. S. Stevenson, H. R. Thompson, K. D. Arvola, K. B. Ghiassi, M. M. Olmstead and A. L. Balch, Isolation of  $CeLu_2N@I_h-C_{80}$  through a Non-Chromatographic, Two-Step Chemical Process and Crystallographic Characterization of the Pyramidalized  $CeLu_2N$  within the Icosahedral Cage, *Chem. Eur. J.*, 2015, **21**, 10362-10368.
26. T. Zuo, C. M. Beavers, J. C. Duchamp, A. Campbell, H. C. Dorn, M. M. Olmstead and A. L. Balch, Isolation and Structural Characterization of a Family of Endohedral Fullerenes Including the Large, Chiral Cage Fullerenes  $Tb_3N@C_{88}$  and  $Tb_3N@C_{86}$  as well as the  $I_h$  and  $D_{5h}$  Isomers of  $Tb_3N@C_{80}$ , *J. Am. Chem. Soc.*, 2007, **129**, 2035-2043.
27. S. Stevenson, J. P. Phillips, J. E. Reid, M. M. Olmstead, S. P. Rath and A. L. Balch, Pyramidalization of  $Gd_3N$  inside a  $C_{80}$  cage. The synthesis and structure of  $Gd_3N@C_{80}$ , *Chem. Commun.*, 2004, DOI: 10.1039/B412338g, 2814-2815.